Liu H, Ayat S, Wrobel R, Zhang C.

Comparative Study of Thermal Properties of Electrical Windings Impregnated with Alternative Varnish Materials.

***In: The 9th International Conference on Power Electronics, Machines and Drives (PEMD 2018)*. 2018, Liverpool, UK: IET.**

Comparative Study of Thermal Properties of Electrical Windings Impregnated with Alternative Varnish Materials

Haipeng Liu*, Sabrina Ayat†, Rafal Wrobel‡, Chengning Zhang*

** National Engineering Laboratory for Electric Vehicles, Beijing Institute of Technology, Beijing, China liuhpbit@gmail.com*
† EEMG, University of Bristol, Bristol, UK, BS8 1UB s.ayat@bristol.ac.uk
‡ Newcastle University, Newcastle upon Tyne, UK, NE1 7RU rafal.wrobel@newcastle.ac.uk

Keywords: Winding impregnation material, varnish, winding homogenization, thermal analysis, PM machine

Abstract

The thermal design-analysis of devices with electrical windings impregnated using varnish materials is frequently challenging. This is due to difficulties in predicting theoretically the equivalent thermal properties for the composite materials, such as impregnated windings, in a reliable manner. The existing approach makes use of the impregnation 'goodness' factor, which allows for imperfections associated with the winding impregnation to be accounted for. This however, requires experimentally derived data from appropriate material samples or machine assemblies. Considering relatively large range of commercially available varnishes, such data is often limited and is not readily accessible. In this investigation, a set of three alternative varnish materials commonly used in impregnation of low voltage electrical windings has been evaluated. To provide better understanding of the material impregnating properties, data from multiple impregnations is also provided. The experimental findings have been supplemented with theoretical analysis on the impregnation 'goodness' and stator-winding contact thermal resistance for a selected winding construction. To highlight the importance of appropriate input thermal material data, a case study machine design is thermally analysed.

1 Introduction

The varnish impregnation has been used in construction of electrical machines and transformers for decades, to guarantee windings with improved electrical insulation, 'good' thermal heat transfer and resilience to mechanical stress [1,2]. When designing a new machine, there are usually a number of multidisciplinary design factors to consider, some of which include the performance and exploitation measures together with in-volume manufacturing cost. The overall cost of employing the varnish impregnation is lower than alternative epoxy resins used to fully encapsulate windings. Also, varnish impregnation is more robust when considering transient thermal overload operation. However, windings potted using epoxy resins have significantly improved heat transfer capability [1,7,15].

A typical electrical winding, impregnated using varnish material is a multi-material composite consisting of conductors, electrical insulation, varnish and various cavities, imperfections related with the impregnation process used [3]. The winding impregnation with an appropriate varnish material enables a cost-effective fabrication process with the impregnation quality to be varied depending on application. For example, dipping or flooding, vacuum or vacuum pressure, or trickle impregnation methods provide different impregnation 'goodness' [2,14]. The equivalent thermal properties of impregnated winding and 'in-situ' winding thermal behaviour have been shown to have a significant impact on dissipative heat transfer from the winding body [1,5]. These clearly have a limiting effect on the machine's power output capability if 'poor' heat transfer path from the winding assembly is realised. Both thermal properties associated with the winding region are strongly depend on the varnish material and impregnation technique used. However, the combined effect of these two factors is notoriously difficult to estimate theoretically [1,5]. This paper employs a combination of theoretical and experimental methods to provide an insight into the thermal behaviour of windings impregnated with alternative varnish materials. A set of three universal vanishes commonly used in construction of low voltage electrical machines and transformers has been selected. To highlight the importance of appropriate input thermal material data, a case study machine design is thermally analysed.

2 Hardware Exemplars

A 10 poles and 12 slots permanent magnet (PM) machine has been designed to meet given requirements of an electric vehicle. An outline of the machine cross section is shown in Fig. 1, and basic machine data includes: 90mm active length, 160mm stator outer diameter, 11,000rpm maximum rotational speed and 62Nm (continuous)/183Nm (transient) torque. The machine has a fixed slot conductor fill factor (45%), a maximum current density (6 A_{rms}/mm^2) for continuous operation and a maximum current density (21 A_{rms}/mm^2) for transient operation considering winding thermal limit. Three alternative universal varnish materials are analysed in this

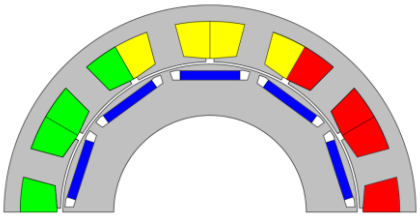

Fig. 1 Cross-section of a half of PM electrical machine

Table I Basic Varnish Material Data

Property	IM-I	IM-II	IM-III
Varnish type	Ultimeg 2000-380 [16]	Elmotherm 073-1010 [17]	ELAN-protect up 142 [18]
Voltage rating, dielectrical strength	- >166 kV/mm [19]	1000V 190℃ >80kV/mm 155℃	1000V 209℃ >235kV/mm 155℃
Solvent	Yes	Yes	No
Insulation class	H (180℃)	H (180℃)	H (180℃)
Curing temperature/time	4 hrs @ 130℃	4 hrs @ 160℃	1 hrs @ 150℃

investigation. The selected varnishes are characterised by different chemical compositions and consequently the physical properties among the materials are expected to be varied. Basic material information is listed in Table I. The available thermal conductivity data for the varnish materials is in range (0.25 – 0.60)W/m·K [1,14,15]. A number of impregnated winding samples have been fabricated and tested to derive the equivalent thermal conductivity following procedure presented in [3]. Here, a winding construction with multi-stranded bundle of round conductors coated with polyamide-imide enamel and wire packing factor $pf = 62\%$ is emulated.

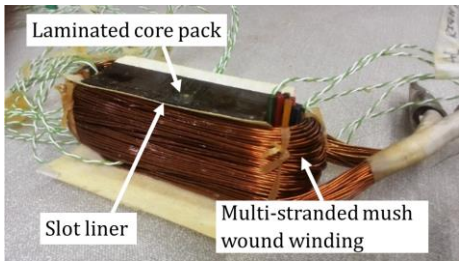

Fig. 2 Instrumented motorette assembly impregnated with IM-III; motorette after the first impregnation.

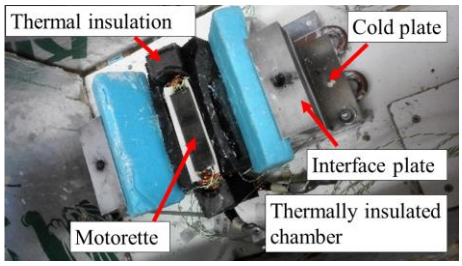

Fig. 3 Experimental set-up showing motorette assembly mounted on a liquid-cooled temperature controlled cold plate and placed in an insulated chamber

Further to the winding material samples, a set of stator-winding segments (motorettes) has been fabricated to evaluate the 'in-situ' thermal properties for the alternative impregnating materials, Fig. 2. It is expected that stator-winding contact thermal resistance will also be affected by the impregnating material. An individual hardware exemplar consists of a laminated stator core pack (NO20, SiFe), a mush-wound coil representative of a concentrated wound winding (Copper) and slot liner (Nomex 410). The coil and stator core are instrumented with several type-K thermocouples. The fully instrumented motorettes are vacuum impregnated with one of the varnish materials and then cured according to the varnish manufacturer data sheet. To avoid the influence of manufacturing variations, all analysed material samples and motorette hardware exemplars have been built with strict control of the assembly and manufacture processes.

3 Experimental Set-up

The thermal conductivity of the cuboidal winding samples is tested using a heat flux approach presented in the authors' previous work [3]. The motorette steady state testing is analogous to that presented in [5] for derivation the 'in-situ' stator-winding thermal properties. The motorette transient testing is analogous to that presented in [6] for transient duty calibration. Fig. 3 presents the experimental setup used in testing the stator-winding segments.

4 Electromagnetic and Thermal Modelling

4.1 Winding Equivalent Thermal Conductivity

A new analytical method is proposed in this paper to estimate the thermal conductivity of the impregnated windings formed with round conductors based on the double-homogenisation approach [7] and [4]. The proposed method homogenises the conductor and conductor insulation first as opposed to the existing approach, where the impregnation material and conductor insulation are dealt with first [3]. The new approach has shown to provide more accurate estimation results.

$$k_a = k_{ci}\frac{(1+\chi)k_c+(1-\chi)k_{ci}}{(1-\chi)k_c+(1+\chi)k_{ci}},\ k_e = k_i\frac{(1+pf)k_a+(1-pf)k_i}{(1-pf)k_a+(1+pf)k_i} \quad (1)$$

where: $\chi = (r_c/(r_c + l_{ci}))^2$, k_a is the equivalent thermal conductivity of homogenized conductor and conductor insulation, k_e is the equivalent thermal conductivity of homogenized winding, χ is the area ratio of the conductor cross-section to wire cross-section, r_c is the conductor radius, l_{ci} is the conductor insulation thickness. Wire packing factor pf is the area ratio of the wire cross-section (including conductor insulation) to the winding window. k_c, k_{ci}, k_i are the thermal conductivity of conductor, conductor insulation, impregnation material, respectively.

A detailed two-dimensional (2D) finite element analysis (FEA) analogous to that presented in [3], with thermal model including individual conductors, conductor insulation and impregnation material has been performed to validate the proposed analytical method. A comparison between the analytical and FE predictions is shown in Fig. 4. It is evident

that the proposed analytical method correlates well with FE data over a wide range of wire packing factors and impregnation thermal conductivities. The thermal conductivity of the varnish materials k_i can be calibrated then using the analytical method and test data from the winding samples testing, k_e, in a computationally efficient way.

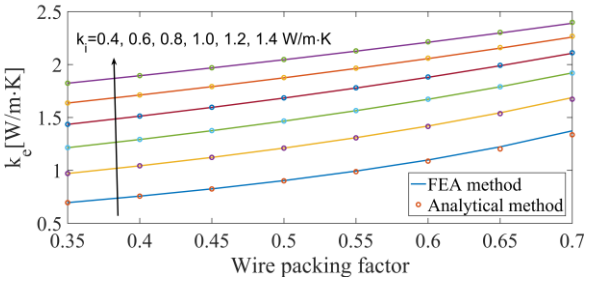

Fig. 4 Calculated winding equivalent thermal conductivity across impregnated conductors versus wire packing factor for alternative impregnation materials; k_c= 385 W/m·K, k_{ci} = 0.26 W/m·K, r_c=0.4 mm, l_{ci}=0.035 mm

The derived thermal conductivity for the analysed varnish materials is listed in Table II. The results show that IM-III has the highest thermal conductivity.

Table II Varnish Thermal Conductivity Derived from Tests on Impregnated Winding Samples

	IM-I	IM-II	IM-III
k_i[W/m·K]	0.71	0.77	1.17

4.2 Stator-winding Contact Thermal Resistance

The approach analogues to that presented in [5] has been employed in this paper. In the thermal FEA of the motorette, the homogenized winding region and stator-winding interface region are modelled separately. It has been assumed here that the equivalent contact thermal conductivity of the stator-winding interface region $k_{ws,eq}$ is transferable from the motorettes to the designed machine, with alike stator-winding construction.

Table III lists the equivalent thermal conductivity of winding region and laminated stator core pack assumed in this analysis [7]. The equivalent thermal conductivity of the winding region is derived based on the material samples. When visually inspecting the impregnation quality of the winding samples and windings of the motorettes, it is evident that for the later ones the impregnation is rather poor with multiple cavities and imperfections. Clearly, the poor 'in-situ' impregnation for the motorettes is more representative of that present in the equivalent in-volume machine manufacture. To illustrate the effect of the multiple impregnation on the 'in-situ' motorette thermal behaviour a thermal data from multiple impregnations has been gathered. It would be rather difficult to separate the influence of the multiple impregnations on the thermal conductivity of the stator-winding contact region and winding itself. Therefore, it has been assumed here that the winding equivalent thermal conductivity for the motorettes does not change at different impregnation stages. The influence of the multiple impregnation is accounted for by the stator-winding interface alone.

Table III The Equivalent Thermal Conductivity of Winding (pf = 60%) and Stator Iron Data Used in the FE 2D Thermal Modelling

Impregnated winding, IM-I	1.56 W/m·K
Impregnated winding, IM-II	1.63 W/m·K
Impregnated winding, IM-III	2.04 W/m·K
Laminated core pack	22.77 W/m·K

4.3 Varnish Volume-Specific Heat Capacity

Transient tests on motorettes impregnated with different varnishes and after multiple impregnation stages indicates that the varnish material and impregnation process have also a significant influence on the winding heat capacity, Fig. 5. This variation in heat capacity will clearly have an effect on thermal behaviour of the motor design case study, in particular for the peak transient operation. A method based on transient thermal modelling of the motorette has been employed here to derive the winding heat capacity and varnish volume-specific heat capacity. This theoretical approach allows to evaluate the influence of multiple impregnations and compare the calculated results with experimentally derived data of heat capacity.

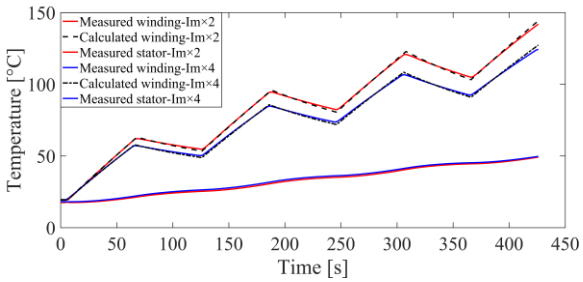

Fig. 5 Calculated averaged winding temperature versus measured averaged winding temperature for motorette impregnated with IM-III. Im×2: winding after second impregnation. Im×4: winding after forth impregnation.

Based on the energy conversion, the winding temperature evolution can be written as:

$$T_w^{k+1} = T_w^k + \frac{t^{k+1}-t^k}{C_w}\left(P_k - \frac{T_w^k - T_{s,measured}^k}{R_{ws}}\right) \quad (2)$$

$$P_k = I_k^2 R_{dc}|T_0(1+\alpha(T_w^k - T_0)) \quad (3)$$

where: R_{ws} is the equivalent thermal resistance between the winding and stator core, C_w is the heat capacity of the winding, P is the winding power loss. T_w and T_s are the averaged winding and averaged stator core pack temperatures, respectively.

A curve fit of the experimental derived data to (2) and (3) has been used to derive C_w and R_{ws}. In the calibration process, only the heat transfer between the winding and stator core pack is considered. This allows to avoid multiple feasible solutions, which usually are present when solving complex thermal

calibration problems and to assure physically representative parameters.

$$C_c = C_{mc}\rho_c V_c, C_{ci} = C_{mci}\rho_{ci}V_{ci}, C_i = C_w - C_c - C_{ci} \quad (4)$$

$$V_i = \frac{V_c+V_{ci}}{pf} - (V_c + V_{ci}), C_{vi} = C_i/V_i \quad (5)$$

where: C_w, C_c, C_{ci}, C_i are the heat capacity values of the winding, conductor in the winding, conductor insulation, and impregnation; C_{mc} and C_{mci} are the mass-specific heat capacity of the conductor and conductor insulation, respectively; ρ_c and ρ_{ci} are the density of the conductor and conductor insulation; V_c and V_{ci} are the volume of the conductor and conductor insulation in the winding, respectively, which can be derived from the wire length, conductor diameter and conductor insulation thickness; pf is the wire packing factor of the winding; V_i is the volume of the impregnation material; C_{vi} is the volume-specific heat capacity of the impregnation material.

4.4 Machine Thermal Model

A 3D lumped-parameter thermal resistance network for the machine design case study has been built to predict its steady state and transient thermal performance and illustrate the influence of alternative varnish materials. The thermal model has been setup using the cuboidal and arc-segment elements [8]. The slot winding and end winding are modelled based on the homogenized winding thermal properties. The thermal properties of other materials, including laminated stator and rotor core packs (M270-35A [9]), permanent magnet (SmCo, 26/10), shaft (Stainless Steel), end cap (Aluminium) and water jacket (Aluminium) are obtained from the available literature [13].

4.5 Machine Power Loss Models

1) Winding Power Loss

In this initial analysis, the ac power loss contribution has been assumed based on the authors previous experience with similar machines/windings builds [10,11]. A functional representation of the winding ac power loss proposed in [10] has been employed here. The $(R_{ac}/R_{dc})_{T_0}$ ratio, which represents increase of the winding dc resistance at ac operation at reference temperature T_0 has been set to be equal to 7 and 3 for the active and end winding regions respectively, at maximum rotational speed. The frequency dependence of $(R_{ac}/R_{dc})_{T_0}$ assuming the resistance limited ac winding effects can be given as:

- winding active region, - winding end region,

$$\left(\frac{R_{ac}}{R_{dc}}\right)|_{T_0} = 6(\frac{f}{f_{max}})^2 + 1, \left(\frac{R_{ac}}{R_{dc}}\right)|_{T_0} = 2\left(\frac{f}{f_{max}}\right)^2 + 1 \quad (6)$$

2) Iron Power Loss and PM Power Loss

The stator, rotor and PM power loss have been derived here using the power loss mapping method provided in [12].

4.6 Torque-Speed Envelope Predictions

A 2D steady state electromagnetic model has been built to derive the electromagnetic torque, T_e, developed by the machine. Both the direct- and quadrature-axis magnetic flux linkages ψ_d and ψ_q have been mapped over a range of current magnitude I_s and current angle γ. The obtained data for $T_e(I_s,\gamma), \psi_d(I_s,\gamma), \psi_q(I_s,\gamma)$ combined with the presented earlier power loss, and thermal models, are used to assess the machine's continuous and transient torque-speed envelopes under maximum torque per amp (MTPA) control. The following performance targets and constraints have been assumed in the analysis:

- maximise torque,

$$T = max\big(T_e(I_s,\gamma)\big) \quad (7)$$

- voltage limit,

$$\omega_e\sqrt{\psi_d^2(I_s,\gamma) + \psi_q^2(I_s,\gamma)} \le U_{lim} \quad (8)$$

- winding temperature limit,

$$T_{ws} \le 165℃ \quad (9) \quad T_{wt} \le 165℃ \quad (10)$$

where: U_{lim} is the voltage limit and $U_{lim} = \frac{U_{dc}}{\sqrt{3}}$, U_{dc} is the dc link voltage (340V), ω_e is the electrical angular speed. T_{ws} is the averaged winding temperature at thermal equilibrium, T_{wt} is the maximum averaged winding temperature during short time transient operation (60 seconds). It is important to note that the transient duty cycle assumes instantaneous change of the rotational speed and torque for the analysed machine. Each of the transient operating points is assessed for the same initial winding temperature, which is equal to the machine housing coolant (70 ℃).

5 Results and discussion

The equivalent thermal conductivity data from testing of the impregnated winding samples shown in Table III suggests that the windings impregnated with solvent based varnishes, IM-I and IM-II, perform in a similar manner. In contrast, the winding impregnated with non-solvent varnish, IM-III, outperforms here the solvent based alternatives by approximately 25% to 30%.

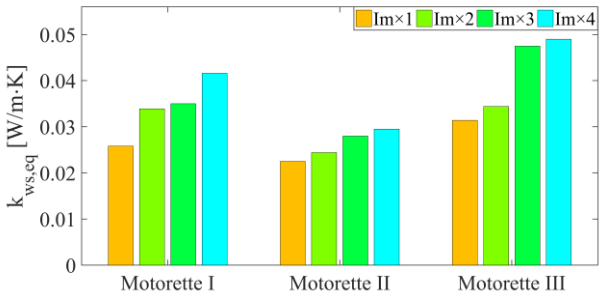

Fig. 6 Stator-winding equivalent contact thermal conductivity

Based on the assumption that the winding equivalent thermal conductivity of the motorettes does not change at different impregnation stages, Fig. 6 presents the derived data for the stator-winding equivalent contact thermal conductivity. The non-solvent varnish, IM-III, provides better stator-winding contact heat transfer at different impregnation stages, which will potentially contribute to improved continuous

torque/power output capability. The solvent based varnish materials perform dissimilarly. After first impregnation, IM-I provides close stator-winding contact heat transfer with IM-II but much better stator-winding contact heat transfer than IM-II after forth impregnation. The difference might result from better material absorption and retention by the winding for IM-I than IM-II. This is evidenced by the specific heat capacity data shown in Fig. 7. Here, an increase of the varnish volume-specific heat capacity for IM-I and IM-II is shown.

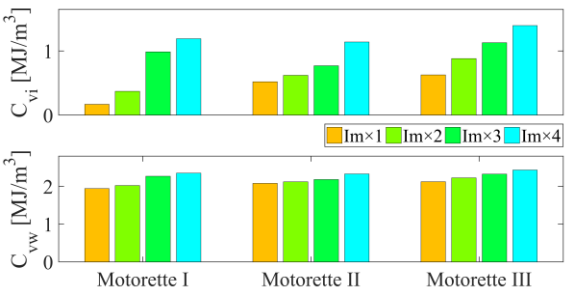

Fig. 7 Varnish (C_{vi}) and corresponding winding (C_{vw}, pf = 60%) equivalent volume-specific heat capacity at different impregnation stages

Fig. 7 presents the equivalent volume-specific heat capacity of the analysed varnish materials and corresponding winding for the consecutive winding impregnation steps, derived from transient thermal tests. As anticipated, the equivalent volume-specific heat capacity for all varnish materials increases with the number of impregnations. This indicates that more varnish material is absorbed and retained by the winding as a result of the multiple impregnations. The trends shown in Fig. 7 suggests that varnish impregnation does not provide good retention of the material.

To illustrate the influence of different varnish materials on performance of the analysed traction electrical machine, an analysis of the complete operating envelope including new European driving cycle (NEDC) has been carried out. Fig. 8 presents the calculated continuous and transient torque-speed envelopes for the machine with windings impregnated with alternative varnish materials. Here, a single winding impregnation has been assumed for all the analysed design variants. The target continuous and transient torque-speed envelopes have been derived based on the initial assumptions regarding the current density and voltage constraints. It is evident here that simple assumptions regarding current density might be insufficient to reliably estimate machine performance. Clearly, design process involving thermal analysis, which is informed with appropriate experimental data is more effective. Fig. 8 shows that the use of alternative varnish materials has some impact in the constant torque region for both continuous and transient torque operating duties. The effect is particularly prominent for low speed range. The influence of the winding-stator heat transfer on the continuous torque output in high speed range is not as obvious as that in low speed range. For the transient operating duty, the machine has enough heat capacity to accommodate for additional ac power losses at reduced current amplitude for the higher speeds within the field weakening region.

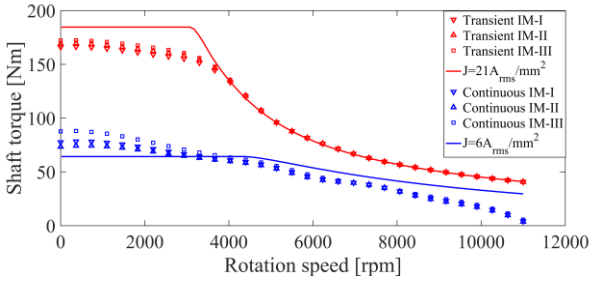

Fig. 8 Torque-speed envelope comparison of the analysed traction motor with winding impregnated using alternative varnish materials; a single impregnation is assumed in this analysis.

A comparison of the continuous and transient torque output at zero speed of the machine with winding impregnated using the alternative varnish materials and consecutive impregnation steps is presented in Fig. 9. The theoretical predictions confirm that machine impregnated with IM-III has the best continuous and transient torque capability for all impregnation steps. The multiple impregnations have moderate impact on the torque output increase for the analysed impregnation variants, 14% (IM-I), 12% (IM-II), 8% (IM-III) and 7% (IM-I), 4% (IM-II), 6% (IM-III) for continuous and transient duty respectively. Here, the improvement between the first and last impregnation is considered.

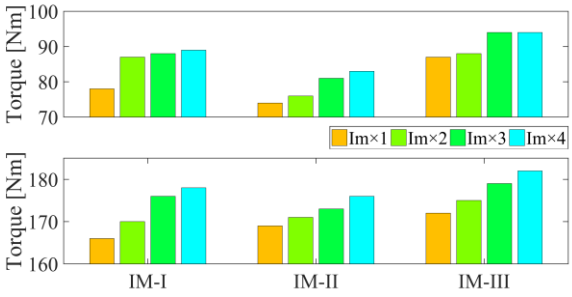

Fig. 9 Continuous and transient torque output at zero speed of the electrical machine impregnated using alternative varnish materials at different impregnation stages.

Table IV Machine Averaged Performance for NEDC

Machine performance	First impregnation			Forth impregnation		
	IM-I	IM-II	IM-III	IM-I	IM-II	IM-III
Averaged efficiency [%]	91.25	91.24	91.28	91.30	91.27	91.33
Winding power loss [Wh]	328.9	330.2	325.6	323.8	326.7	321.7
Winding temp. rise [°C]	76.8	77.5	69.6	64.7	69.6	60.6

In the analysis, the influence of winding temperature on winding dc loss and ac loss is considered. The PM flux is assumed to be not changed with PM temperature. Also, the iron loss and PM loss are assumed to be independent of temperature. Table IV lists the averaged motor performance.

The calculated results suggest that machine with IM-III impregnation exhibits lower averaged winding temperature rise over the operating duty cycle than that of the design variants with IM-I and IM-II varnishes. Approximately, 10% difference in the averaged winding temperature rise has been observed here. All design variants show improvement of in the averaged winding temperature when comparing data from the first and last impregnation steps, 15.8%, 10.2%, 12.9% for IM-I, IM-II, IM-III, respectively.

6 Conclusions

This paper presents results from a comparative study of thermal properties of electrical windings impregnated with alternative varnish materials. A new more reliable analytical method for estimating the equivalent thermal conductivity of impregnated windings formed with round conductors has been proposed in this paper. Using the proposed method, a set of thermal conductivity data for alternative varnish materials has been derived from tests on impregnated winding hardware. The stator-winding equivalent contact thermal conductivity and winding/varnish volume-specific heat capacity has also been found from tests on the motorette hardware.

The results show that the winding impregnated with non-solvent varnish IM-III performs better than windings with solvent alternatives, IM-I and IM-II. The multiple impregnation allows for both the steady state and transient winding temperature rise to be reduced for all analysed varnish materials. The most prominent increase of the stator-winding heat transfer capabilities appears as a result of the first impregnation. Through the analysis of electrical machine impregnated with alternative varnish materials based on the calibrated varnish thermal properties, the electrical machine impregnated with IM-III has the best performance among the analysed design variants. The performance improvement is particularly evident in the low speed region of the torque-speed envelope. The peak transient operation shows negligible difference for the machine design variants with alternative varnish materials. The performance analysis for NEDC has shown that machine design with IM-III impregnation has the lowest averaged winding temperature rise. However, the theoretical predictions do not show distinct deviation when comparing the power loss or efficiency data over the assumed duty cycle. Also, the measured data indicates, that multiple impregnation is an effective way to increase the transient/continuous torque-speed envelope, especially in the low speed region. Moreover, the multiple impregnation enables to decrease the transient winding temperature, but its impact on the machine efficiency is less pronounced. The non-solvent varnish, IM-III shows its advantage for multiple impregnation, due to its much shorter curing time.

The non-solvent varnish, IM-III has been selected as the impregnation material for the traction motor thermal design and optimization. The multiple impregnation, e.g. double impregnation, might be a good compromise for the winding manufacture when considering the performance measures and manufacture time and associated cost.

References

[1] S. Nategh, A. Krings, O. Wallmark, and M. Leksell, "Evaluation of Impregnation Materials for Thermal Management of Liquid-Cooled Electric Machines," *IEEE Transactions on Industrial Electronics*, vol. 61, no. 11, pp. 5956–5965, Nov. 2014.

[2] A. Boglietti, A. Cavagnino, and D. A. Staton, "Thermal sensitivity analysis for TEFC induction motors," in *Second International Conference on Power Electronics, Machines and Drives (PEMD 2004).*, 2004, vol. 1, p. 160–165 Vol.1.

[3] N. Simpson, R. Wrobel, and P. H. Mellor, "Estimation of Equivalent Thermal Parameters of Impregnated Electrical Windings," *IEEE Transactions on Industry Applications*, vol. 49, no. 6, pp. 2505–2515, Nov. 2013.

[4] L. Idoughi, X. Mininger, F. Bouillault, L. Bernard, and E. Hoang, "Thermal Model with Winding Homogenization and FIT Discretization for Stator Slot," *IEEE Transactions on Magnetics*, vol. 47, no. 12, pp. 4822–4826, Dec. 2011.

[5] R. Wrobel, S. J. Williamson, J. D. Booker, and P. H. Mellor, "Characterizing the in situ Thermal Behavior of Selected Electrical Machine Insulation and Impregnation Materials," *IEEE Transactions on Industry Applications*, vol. 52, no. 6, pp. 4678–4687, Nov. 2016.

[6] J. Godbehere, R. Wrobel, D. Drury, and P. H. Mellor, "Experimentally Calibrated Thermal Stator Modelling of AC Machines for Short-Duty Transient Operation," *IEEE Transactions on Industry Applications*, vol. PP, no. 99, pp. 1–1, 2017.

[7] R. Wrobel, S. Ayat, and J. L. Baker, "Analytical methods for estimating equivalent thermal conductivity in impregnated electrical windings formed using Litz wire," in 2017 IEEE International Electric Machines and Drives Conference (IEMDC), 2017, pp. 1–8.

[8] N. Simpson, R. Wrobel, and P. H. Mellor, "A General Arc-Segment Element for Three-Dimensional Thermal Modeling," IEEE Transactions on Magnetics, vol. 50, no. 2, pp. 265–268, Feb. 2014.

[9] J. L. Baker, R. Wrobel, D. Drury, and P. H. Mellor, "A methodology for predicting the thermal behaviour of modular-wound electrical machines," in 2014 IEEE Energy Conversion Congress and Exposition (ECCE), 2014, pp. 5176–5183.

[10] R. Wrobel, D. E. Salt, A. Griffo, N. Simpson, and P. H. Mellor, "Derivation and Scaling of AC Copper Loss in Thermal Modeling of Electrical Machines," IEEE Transactions on Industrial Electronics, vol. 61, no. 8, pp. 4412–4420, Aug. 2014.

[11] P. H. Mellor, R. Wrobel, and N. McNeill, "Investigation of Proximity Losses in a High Speed Brushless Permanent Magnet Motor," in Conference Record of the 2006 IEEE Industry Applications Conference Forty-First IAS Annual Meeting, 2006, vol. 3, pp. 1514–1518.

[12] J. Goss, M. Popescu, D. Staton, R. Wrobel, J. Yon, and P. Mellor, "A comparison between maximum torque/ampere and maximum efficiency control strategies in IPM synchronous machines," in 2014 IEEE Energy Conversion Congress and Exposition (ECCE), 2014, pp. 2403–2410.

[13] Pyrhonen Juha, Tapani Jokinen, and Valeria Hrabovcova. Design of rotating electrical machines. John Wiley & Sons, 2008.

[14] http://www.elantas.com/fileadmin/elantas/companies/europe/downloads/Impregnation_Materials_Elan-protect_english.pdf (visited on 13/07/2017)

[15] http://www.lakeshore.com/Documents/LSTC_epoxygv_l.pdf (visited on 13/07/2017)

[16] https://www.aev.co.uk/ (visited on 30/06/2017)

[17] http://www.wes.uk.com/files/87.pdf (visited on 11/07/2017)

[18] http://www.elantas.com/europe/products/impregnating-materials/applications/dip-hot-dip.html (visited on 11/07/2017)

[19] http://www.bew.com.au/files/380%20data1.pdf (visited on 13/07/2017)